The oncogenic miR-27a/BTG2 axis promotes obesity-associated hepatocellular carcinoma by mediating mitochondrial dysfunction

Qi SU[1,#], Zi-Xin XU[2,#], Min-Li XIONG[3], Hui-Yi LI[4], Ming-Yi XU[4,*], Sheng-Zheng LUO[2,*]

[1]Department of Critical Care Medicine, Shanghai General Hospital, Shanghai Jiao Tong University School of Medicine, Shanghai, China; [2]Department of Gastroenterology, Shanghai General Hospital, Shanghai Jiao Tong University School of Medicine, Shanghai, China; [3]Outpatient Department of Shanghai University of International Business and Economics, Shanghai, China; [4]Department of Gastroenterology, Shanghai East Hospital, Tongji University School of Medicine, Shanghai, China

*Correspondence: luoshengzheng2007@163.com; xumingyi2014@163.com
#Contributed equally to this work.

Obesity is closely related to the initiation and development of hepatocellular carcinoma (HCC). The regulatory mechanism of obesity-associated HCC remains unclear. HepG2 cells treated with palmitic acid (PA) and diethylnitrosamine (DEN)-induced HCC mice fed a high-fat diet (HFD) were established. The expression of miR-27a and B-cell translocation gene 2 (BTG2) mRNA and protein were detected via qPCR and western blotting. Prediction software and luciferase assays were employed to verify the miR-27a/BTG2 axis. The biological effects of HepG2 cells were evaluated with ORO staining, MTT assays, Transwell assays, Mito-Timer, and Mito-SOX staining. Significantly upregulated miR-27a and downregulated BTG2 mRNA and protein were observed in HepG2 cells and liver tissues of HCC mice. Overexpressing miR-27a (mi-miR-27a) markedly promoted cellular lipid accumulation, proliferation, and invasion, accompanied by aggravated mitochondrial dysfunction (increased fading and ROS products of mitochondria) in HepG2 cells. Additionally, these effects were further reinforced in HepG2 cells treated with mi-miR-27a and PA. BTG2 was identified as a direct target and was negatively regulated by miR-27a. Similarly, BTG2 knockdown (sh-BTG2) had effects identical to those of mi-miR-27a on HepG2 cells. Additionally, PA evidently enhanced these effects of sh-BTG2 in HepG2 cells. Moreover, BTG2 overexpression effectively reversed the effects of miR-27a, including lipotropic and oncogenic effects, and simultaneously promoted mitochondrial imbalance in HepG2 cells. Thus, obesity-associated miR-27a acts as an oncogene to promote lipid accumulation, proliferation, and invasion by negatively regulating BTG2-mediated mitochondrial dysfunction in HCC.

Key words: hepatocellular carcinoma (HCC), microRNA-27a (miR-27a), B-cell translocation gene 2 (BTG2), obesity, mitochondria

Hepatocellular carcinoma (HCC) poses a major public health problem with a rapidly increasing incidence and death rate [1]. Obesity is rapidly becoming a global issue with a substantial risk factor for tumorigenesis, a particularly independent risk factor for HCC [2, 3]. Moreover, obesity-related HCC further evolves in a subset of nonalcoholic fatty liver disease (NAFLD), which is also related to the prevalence of obesity [4]. In HCC, a high-fat diet or exposure to palmitic acid (PA) could aggravate HCC development [5, 6]. Palmitate suppressed cell activity, induced lipid accumulation, and elevated reactive oxygen species (ROS) production in HepG2 cells [7]. Multiple mechanisms underlying obesity in hepatocarcinogenesis involve cell signaling and neural and immunological modifications [8]. Understanding the key molecular features of HCC and offering novel mechanistic insights into therapeutic strategies remain essential tasks.

Currently, a rising family of molecules, adipocyte-derived microRNAs (miRNAs, miRs), have become a research hotspot due to their regulatory role in HCC [9]. miR-27a has been recognized as a lipogenic regulator and adipocyte tissue-derived miRNA [10]. Obesity-associated miR-27a can promote metastasis of HCC cells [11]. Furthermore, mitochondrial dysfunction was also found to be closely related to ectopic expression of miR-27a [12]. Also, to explore the signal of obesity-associated miR-27a, we also focus on the target genes. B-cell translocation gene 2 (BTG2), one of the targets of miR-27a, was originally identified as a member of the anti-proliferative gene family. BTG2 has been implicated in HCC development, including cell proliferation, migration, and invasion [13].

Therefore, our work aims to mechanistically investigate the obesity-associated miR-27a modification of mitochondrial

function in HCC. In this study, we revealed novel insights into the obesity-associated miR-27a/BTG2 axis, which promotes HCC development by influencing mitochondrial function.

Materials and methods

Animal experiments. A total of 20 C57BL/6 mice (8 weeks old, male; Shanghai SLAC Laboratory Animal Co. Ltd., Shanghai, China) were randomly divided into 2 groups (each group n=10) fed a normal chow diet (ND, 10 kcal% fat, 20% protein, and 70% carbohydrate) or a high-fat diet (HFD, 60% fat, 20% protein, and 20% carbohydrate) for 28 weeks (Trophic Animal Feed High-tech Co. Ltd., Nantong, Jiangsu, China). All mice were injected intraperitoneally with diethylnitrosamine (DEN 45 mg/kg, Sigma-Aldrich, St. Louis, MO, USA) to induce HCC over 16–36 weeks. Mice were euthanized one week after the last injection of DEN by cervical dislocation under anesthesia with 350 mg/kg chloral hydrate (10%, abdominal injection). Mice were checked for complete cardiac arrest and pupil dilation to confirm death and then their blood samples and liver tissue samples were collected for subsequent analysis. Tumor and adjacent liver tissues were excised and rapidly frozen for subsequent assays. This study was approved by the committee for animal use of the Shanghai General Hospital.

H&E staining. Formalin-fixed mouse liver tissue samples were embedded in paraffin, cut into 5 μm thick sections, and then stained with hematoxylin-eosin. The images were obtained using an inverted microscope (Leica Microsystems, Wetzlar, Germany). The tumor size was semi-quantified by calculating the percentage of tumor area in the total area of each image.

Cell line culture and treatment. A transformed human liver epithelial-2 cell line (THLE-2; Bluefbio Shanghai Biotechnology Development Co. Ltd, Shanghai, China) and human liver cancer cell lines (HCCLM3 and HepG2; Chinese Academy of Sciences Shanghai Cell Biology Institute, Shanghai, China) were used, and cultured in Dulbecco's modified Eagle's medium (DMEM; Gibco, Grand Island, NY, USA). The cell lines used in our study were authenticated by STR profiling (see suppl. STR profile file).

Primary hepatocytes (PHCs) were isolated from C57BL/6 mice using two-step collagenase perfusion according to a previously described protocol [14]. Briefly, collagenase perfusion was performed through the portal vein of anesthetized mice with 50 ml of perfusion buffer and 5,000 U of collagenase I (Roche, Basel, Switzerland) at 37 °C. The liver was aseptically removed to a sterile 10 cm cell culture dish containing 20 ml of ice-cold perfusion buffer without collagenase. The excised liver was cut, and hepatocytes were dispersed via aspiration with a large-bore pipette, followed by filtration through a 70 μm cell strainer (Thermo Fisher Scientific Inc., Waltham, MA, USA) into a 50 ml centrifuge tube before centrifugation at 50 g for 2 min at 4 °C. The cells were washed and resuspended in an M199 medium (Gibco).

Cells were treated with 200–400 μM palmitic acid (PA, Sigma-Aldrich) for 24–48 hours in a medium to induce high-fat conditions.

Cell transfection. A pcDNA 3.1 plasmid (GenePharma Co., Ltd, Shanghai, China) containing the amplified cDNA of BTG2 was constructed to overexpress BTG2 (ov-BTG2). Short hairpin RNA (shRNA) against BTG2 was cloned into a pENTR-U6 plasmid to knock down BTG2 (sh-BTG2, GenePharma), and the plasmid carrying a nontargeting sequence was used as a negative control (sh-NC). Cells were transfected with miR-27a mimic (mi-miR-27a, GenePharma) to upregulate miR-27a or a negative control miRNA (mi-NC). Cell transfection was performed according to the Lipofectamine 3000 (Invitrogen, Carlsbad, CA, USA) protocol. Detailed information on the oligonucleotides is displayed in Supplementary Table S1.

Quantitative real-time PCR (qPCR). Total RNA was extracted using TRIzol® (Thermo Fisher Scientific Inc.) and a miRNA easy mini kit (Qiagen, Düsseldorf, Germany). U6 and GAPDH were employed as endogenous controls. Specific stem-loop primers and a TaqMan® MicroRNA Reverse Transcription kit (Thermo Fisher Scientific Inc.) were used to reverse transcribe the samples of total RNA (10 ng) into cDNA. In a 15 μl reaction volume, mixtures were incubated for 30 min at 16 °C, 30 min at 42 °C, and 5 min at 85 °C, and held at 4 °C. For mRNA, first-strand cDNA was reverse transcribed from RNA (25 °C, 5 min; 42 °C, 15 min; 85 °C, 5 min) using a Hifair® II 1st Strand cDNA Synthesis Kit (Yeasen Bio Technologies Co. Ltd., Shanghai, China). Following the RT reaction, qPCR was carried out with an ABI 7300 Real-Time PCR system (Bio-Rad Lab. Inc., CA, USA) and SYBR Green (Invitrogen) according to the manufacturer's protocol. The thermocycling conditions were 95 °C for 5 min, followed by 40 cycles of 95 °C for 10 s, and 60 °C for 30 s in a 20 μl reaction volume. The relative levels of each miRNA and mRNA were determined by the 2−ΔΔCq method. All results were normalized to U6 or GAPDH expression levels, which were analyzed simultaneously. The sequences of primers (Sangon Biotech Co. Ltd, Shanghai, China; Sinotech Genomics Co. Ltd, Shanghai, China), GenBank accession numbers, and the expected sizes for qPCR are shown in Supplementary Table S2.

Western blotting. Total protein was extracted from cells or tissues using RIPA buffer (Beyotime Institute of Biotechnology, Shanghai, China). A BCA protein assay (Beyotime Institute of Biotechnology) was used to quantify protein concentration. Then, 10% SDS-PAGE was used to separate the proteins, which were subsequently transferred onto PVDF membranes (Thermo Fisher Scientific Inc.) for 90 min at a current of 300 mA. The membranes were blocked with 5% nonfat milk for 1 h at room temperature and incubated with primary antibodies targeting the following proteins overnight at 4 °C: BTG2 (1:2000; CAT:sc-517187, Santa Cruz Biotechnology, Santa Cruz, CA, USA) and GAPDH (1:1000,

CAT:sc-2004, Santa Cruz Biotechnology). On the next day, the PVDF membranes were incubated with a secondary antibody (HRP-IgG, 1:10000; CAT:sc-2004, Santa Cruz Biotechnology) at room temperature for 2 h. Subsequently, the protein bands were observed using an enhanced chemiluminescence detection system (Amersham Imager 600, General Electric Company, Boston, USA), and detection of band grey values was performed using ImageJ 1.8.0 (Rawak Software Inc., Stuttgart, Germany).

MTT assay. Cell proliferation and viability were measured using 3-(4,5-dimethylthiazol-2-yl)-2,5-diphenyltetrazolium bromide (MTT, Sigma-Aldrich). An absorbance wavelength of 570 nm was used to assess cell proliferation via a spectrophotometric plate reader (Thermo Fisher Scientific Inc.). Quantification was determined by the optical density (OD) value.

Transwell assay. After treatment, cells were collected for further cultivation in a Transwell chamber (Corning Incorporation, Corning, NY, USA). The upper chamber was coated with Matrigel (BD Bioscience, San Jose, CA, USA), and the lower chamber was filled with DMEM containing 10% fetal bovine serum (Gibco). Cells were cleared from the upper member with a sterilized cotton swab after incubation for 48 h, and then, cells in the lower chamber were fixed with 4% paraformaldehyde. The number of invading cells was calculated under a light microscope after staining with 0.5% crystal violet solution.

Bioinformatics analysis. To probe the molecular mechanisms underlying miRNA, we used miRNA target prediction bioinformatics software: Target Scan Human 8.0 (http://www.targetscan.org) and miRDB (http://mirdb.org) to search for the candidate targets of miR-27a.

Luciferase assay. Luciferase assays were carried out using a Dual Luciferase Reporter Assay Kit (Promega, Madison, WI, USA) according to the manufacturer's protocol. Briefly, complementary DNA fragments containing wild-type or mutant BTG2 3'UTR binding sites (sequence details are given in Supplementary Table S3) were cloned downstream of the luciferase gene in a pMIR-GLO reporter vector. Then, luciferase activity was determined with a luciferase kit.

Oil Red O (ORO) staining. Cells were fixed in 4% paraformaldehyde for 10 min followed by washing with PBS and then with 60% isopropanol. Freshly diluted ORO solution (Sigma-Aldrich) was used to stain cells for 30 min. After being washed with PBS, the cells were photographed under a light microscope.

Mito-SOX staining. The levels of reactive oxygen species (ROS) were determined through Mito-SOX staining according to the manufacturer's instructions. Overall, HepG2 cells were rinsed with PBS and incubated with 5 mM Mito-SOX (Invitrogen) for 15 min at 37 °C in the dark. Then, the cells were washed with PBS, the samples were photographed via fluorescence microscopy, and the fluorescence (IF) intensity was quantified using ImageJ software (National Institutes of Health, Bethesda, MD, USA).

Mito-Timer staining. Mito-Timer plasmid (cat. no. 50547; Biovector NTCC Inc., Beijing, China) was transfected into HepG2 cells using Lipofectamine 3000 following the manufacturer's recommendations. Cells expressing Mito-Timer fluorescent proteins were imaged using fluorescence microscopy to determine the Mito-Timer ratio metric shift (IF ratio of green vs. red) as an indication of mitochondrial aging and damage.

Statistical analysis. All the results shown are based on repeated experiments. Values in bar and curve graphs are expressed as the mean and standard errors. SPSS 25.0 (SPSS, Version X; IBM, Armonk, NY, USA) was used for statistical analysis. A p-value <0.05 was set to indicate a statistical significance. Unpaired Student t-test was used to analyze the differences between the two groups, one-way ANOVA followed by Student-Newman-Keuls analysis was used for a comparison of multiple groups. Besides, although some data of two treatments were presented in one graph, our data were independent comparisons of a single factor and did not involve the interaction of two factors, so there was no two-way analysis of variance.

Results

miR-27a was significantly elevated in liver cancer cells and tissues, especially in obese conditions. To thoroughly investigate the role of miRNAs in HCC, we focused on miR-27a because it was reported as an oncogene in HCC and as an obesity-associated miRNA. miR-27a expression was increased approximately 2–3-fold in human liver cancer cells (HepG2 and HCCLM3) compared to THLE-2 cells (p<0.05, Figure 1A). In addition, compared to control HepG2 cells (Ct group), miR-27a expression was obviously enhanced in PA-treated HepG2 cells in a dose-dependent manner (p<0.05, Figure 1A).

Moreover, to evaluate the expression of miR-27a in hepatic tissues, we established DEN-induced HCC mice fed a ND and HFD (Figure 1B). In ND adjacent liver tissues, less inflammatory cell infiltration and steatosis were observed; while in HFD adjacent liver tissues, extensive steatosis was seen. In ND tumor tissues, lymphocytes and neutrophils infiltration without obvious necrosis could be seen. In HFD tumor tissues, more extensive necrosis, obvious granulocytic infiltration, and obvious steatosis also could be found. Compared with the ND tumor tissues, the percentage of tumor size was significantly increased in the HFD tumor tissues (ND tumor tissues vs. HFD tumor tissues: 25% vs. 75%, p<0.05, Figure 1B). Consistently, we found that the miR-27a expression was clearly enhanced in tumor tissues compared to adjacent tissues in ND and HFD mice. In addition, the most elevated miR-27a levels were present in HCC tissues from the HFD group (Figure 1B). Thus, miR-27a was dramatically upregulated in liver cancer cells and tissues, and its expression reached a peak level in HCC with obesity.
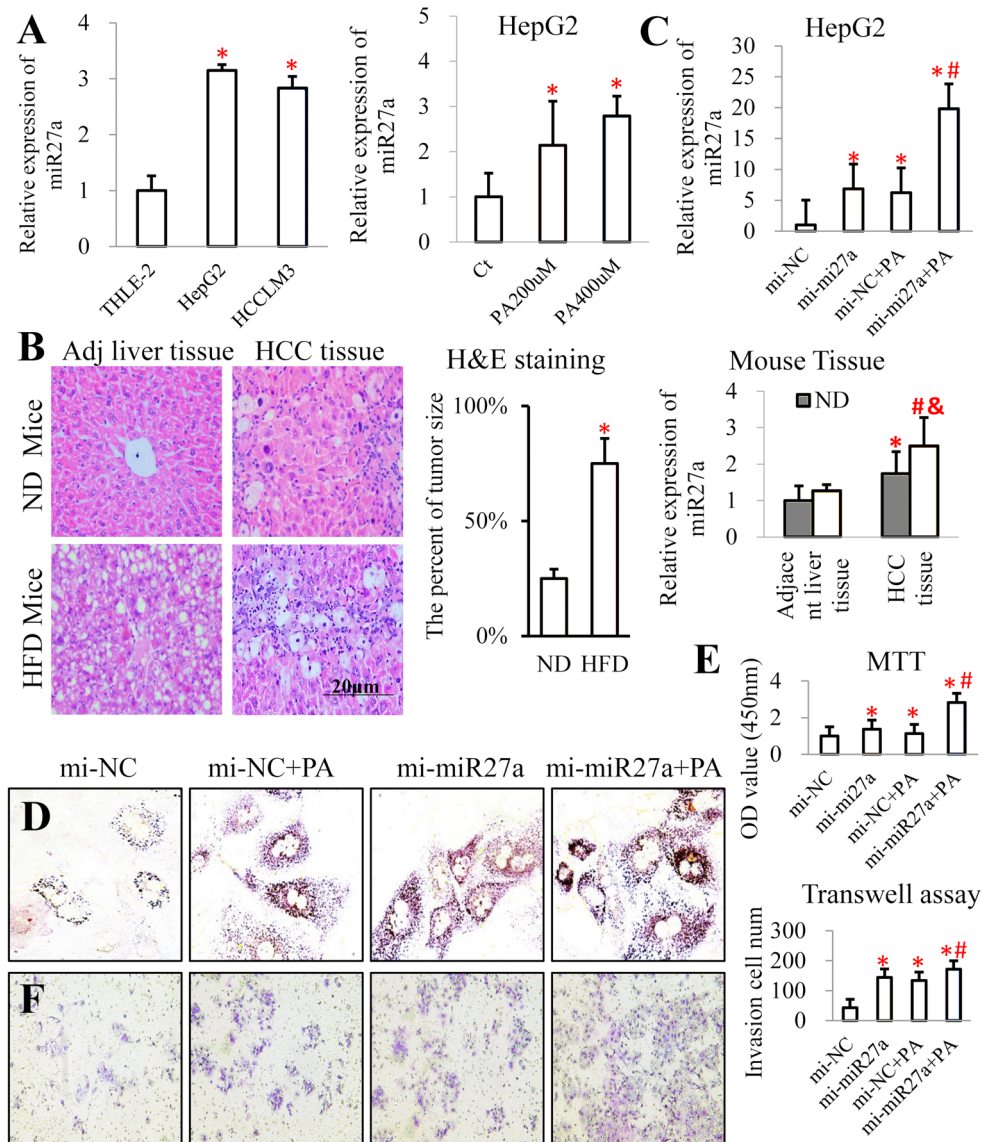
Figure 1. Obesity-associated miR-27a was highly upregulated in liver cancer cells and tissues and obviously promoted cellular lipid accumulation, proliferation, and invasion in HCC. A) Relative miR-27a expression was assessed via qPCR in different cell lines (THLE-2, HepG2, and HCCLM3, upper panel) and in HepG2 cells treated with BSA (Ct group) or PA (200 and 400 μM, lower panel). *Indicates THLE-2 cells vs. the Ct group, p<0.05 **B)** HCC mice were fed a ND or HFD (each group, n=10). H&E staining and relative miR-27a expression were examined by qPCR in HCC tissues and adjacent tissues. The unit is % of tumor size measurement. *Indicates vs. adjacent liver tissue in the ND group, p<0.05; #indicates vs. adjacent liver tissue in the HFD group, p<0.05; & indicates vs. HCC tissue in the ND group, p<0.05. **C–F)** mi-NC, mi-miR-27a, mi-NC+PA, and mi-miR27a+PA groups were established in HepG2 cells and PHCs. **C)** Relative miR-27a expression was examined via qPCR in HepG2 cells. **D)** Images of lipid accumulation visualized using ORO staining in PHCs are presented. **E)** Cellular viability was examined via MTT assays in HepG2 cells. **F)** Invasion was determined by Transwell assays in HepG2 cells. *Indicates vs. the mi-NC group, p<0.05, #indicates vs. the mi-miR-27a group, p<0.05

Obesity-associated miR-27a upregulation significantly promoted cellular lipid accumulation, proliferation, and invasion in liver cancer cells. To investigate the molecular mechanisms of obesity-associated miR-27a *in vitro*, four groups of HepG2 cells and PHCs were established (mi-NC, mi-miR-27a, mi-NC+PA, mi-miR-27a+PA groups). In HepG2 cells, miR-27a mimic (overexpression of miR-27a) or PA treatment significantly upregulated the expres-

sion of miR-27a (mi-miR-27a vs. mi-NC group: 6.87-fold; mi-NC+PA vs. mi-NC group: 6.23-fold; Figure 1C), while miR-27a mimic combined with PA treatment caused the highest expression of miR-27a (mi-miR-27a+PA vs. mi-miR-27a group: 2.89-fold; mi-miR-27a+PA vs. mi-NC group: 19.8-fold; Figure 1C). Compared to PHCs or HepG2 cells in the mi-NC group, more lipid accumulation was observed in cells in the mi-NC+PA and mi-miR-27a groups, while

the most obvious lipid accumulation was present in cells in the mi-miR-27a+PA group (Figure 1D, Supplementary Figure S1A). Compared with HepG2 cells in the mi-NC group, mi-miR-27a or PA treatment significantly increased cell viability and growth (Figure 1E) and markedly increased cell invasion (Figure 1F). The most reinforced invasion and proliferation ability were displayed in mi-miR-27a+PA cells (Figures 1E, 1F). These data reveal that obesity-associated miR-27a upregulation can stimulate lipid accumulation, proliferation, and invasion in liver cancer cells.

Obesity-associated miR-27a notably disturbed mitochondrial function in liver cancer cells. Mitochondria play an important role in maintaining cell homeostasis, and the accumulation of dysfunctional mitochondria was found to be associated with liver tumorigenesis [15]. To evaluate the impact of obesity-associated miR-27a on mitochondrial function in HepG2 cells, Mito-Timer proteins and Mito-SOX IF staining were employed. Mito-Timer proteins were used to monitor real-time mitochondrial biogenesis, turnover, and aging with an age-dependent shift in IF from green to red over time [16]. While increased red IF (indicating damaged and old mitochondria) could be seen in mi-miR-27a cells and mi-NC+PA cells, enhanced green IF (indicating healthy and young mitochondria) was present in mi-NC cells (Figure 2A). Moreover, mi-miR-27a+PA cells showed the most increased red IF (Figure 2A). Thus, mi-miR-27a and PA accelerated mitochondrial senescence and impairment, which could be further enhanced by mi-miR-27a+PA. Mito-SOX is a cell-permeable dye that can exhibit red IF by targeting mitochondrial ROS products [17]. Consistently, Mito-SOX staining revealed that mi-miR-27a and mi-NC+PA cells showed amplified red IF compared to mi-NC cells (Figure 2B). In addition, mi-miR-27a+PA induced the greatest red IF accumulation in HepG2 cells (Figure 2B). This result indicates that mi-miR-27a or PA can induce increased oxidative stress reactions in mitochondria, while mi-miR-27a+PA caused the highest level. Collectively, we hypothesized that obesity-associated miR-27a upregulation exerted the key effect of disturbing mitochondrial function, possibly resulting in oncogenic effects in liver cancer cells.

BTG2 was a key target and was negatively regulated by obesity-associated miR-27a in HCC. To explore the regulated signaling underlying obesity-associated miR-27a, we focused on four downstream targets of miR-27a [BTG2, forkhead box protein O1 (FOXO1), insulin-like growth factor-1 (IGF-1), and SMAD family member 2 (SMAD2)], which were reported to be involved in cellular proliferation or migration against miR-27a in tumors [18-21]. mi-miR-27a robustly inhibited the expression of BTG2, IGF-1, FOXO1, and SMAD2 in HepG2 cells (Figure 3A). Interestingly, PA treatment only obviously suppressed the expression of BTG2 mRNA, but there was no difference in IGF-1, FOXO1, and SMAD2 expression in HepG2 cells (Figure 3A). Furthermore, the greatest decrease in BTG2 mRNA expression was observed in HepG2 cells in the mi-miR-27a+PA

group (Figure 3A). Thus, it was reasoned that BTG2 might be an important target of obesity-associated miR-27a in HCC. BTG2 mRNA and protein expression was distinctly reduced in human liver cancer cells (HepG2 and HCCLM3) compared to THLE-2 cells (Figure 3B). Additionally, BTG2 mRNA and protein expression were notably reduced in HCC tissues compared with adjacent liver tissues in ND and HFD mice (Figure 3B). The lowest BTG2 mRNA and protein levels were observed in tumoral tissues of HFD mice (Figure 3B). These data indicate that BTG2 mRNA and protein expression was clearly decreased in liver cancer cells and tissues, especially under obese conditions.

BTG2, a well-known antiproliferation gene, negatively regulates growth by inhibiting the cell cycle progression in liver cancer [22]. BTG2 was also reported to suppress lipid accumulation and protect against mitochondrial damage [23, 24]. Therefore, we focused on BTG2 for further study. Two binding sites for miR-27a (nt361-368 and nt1832-1838) were identified in the 3'-untranslated region (3'UTR) of BTG2 using target prediction programs (miRDB and Target Scan, Figure 3C). Furthermore, luciferase reporters containing BTG2-wt (wild-type BTG2) and BTG2-mut (mutant-type BTG2) were constructed and used to transfect mi-NC or mi-miR-27a HepG2 cells. Only the transfection with miR-27a suppressed the luciferase activities of BTG2-wt (Figure 3D). Therefore, BTG2 was identified as an important target and was found to be negatively regulated by obesity-associated miR-27a in HCC.

Inhibition of BTG2 evidently promoted lipid accumulation, proliferation, and invasion in obesity-related liver cancer cells. To validate the biological functions of BTG2, four groups of PHCs and HepG2 cells were constructed: shRNA negative control (sh-NC), BTG2 knockdown (sh-BTG2), sh-NC+PA, and sh-BTG2+PA. Through ORO staining, sh-BTG2 or PA treatment was found to lead to a greater enrichment of lipid accumulation in PHCs and HepG2 cells compared to their control cells (Figure 4A, Supplementary Figure S1B). The most lipid accumulation was seen in the sh-BTG2+PA group cells (Figure 4A, Supplementary Figure S1B). Consistently, cellular proliferation (Figure 4B) and the number of invading cells (Figure 4C) were evidently increased by sh-BTG2 or PA treatment. Moreover, sh-BTG2+PA treatment had the greatest effect on stimulating cell proliferation (Figure 4B) and invasion (Figure 4C). Thus, inhibition of BTG2 remarkably accelerated lipid accumulation, proliferation, and invasion in obesity-related liver cancer cells.

Suppression of BTG2 resulted in striking mitochondrial dysfunction in obesity-related liver cancer cells. BTG2 has been reported to be responsible for protection against mitochondrial damage; thus, we hypothesized that sh-BTG2 may induce mitochondrial dysfunction in obesity-related liver cancer cells. In the Mito-Timer analysis, sh-BTG2 or PA treatment dramatically promoted red IF accumulation (indicating senescent and impaired mitochondria, Figure 5A), while sh-NC treatment mainly induced

green IF (indicating healthy mitochondria, Figure 5A). The most intense red IF was seen in the cells in the sh-BTG2+PA group (Figure 5A). Therefore, sh-BTG2 or PA can provoke mitochondrial fading and damage, which can be markedly enhanced by sh-BTG2+PA. Consistently, evidently increased red IF (indicating more mitochondrial ROS products) was exhibited after Mito-SOX staining of HepG2 cells in the sh-BTG2 and sh-NC+PA groups compared to that in cells in the sh-NC group (Figure 5B). In addition, the greatest red IF was observed in sh-BTG2+PA cells (Figure 5B). Thus, more

redoubtable oxidative stress reactions in mitochondria were induced by sh-BTG2 or PA, and the highest level was caused by sh-BTG2+PA. Therefore, suppressing BTG2 may aggravate obesity-related HCC, chiefly by injuring mitochondrial function *in vitro*.

Obesity-associated miR-27a exacerbated HCC mainly by negatively regulating BTG2-related mitochondrial impairment *in vitro*. To gain further insight into the obesity-associated miR-27a-BTG2 axis in the HCC biological process, we constructed two groups of PHCs and HepG2 cells: mi-miR-
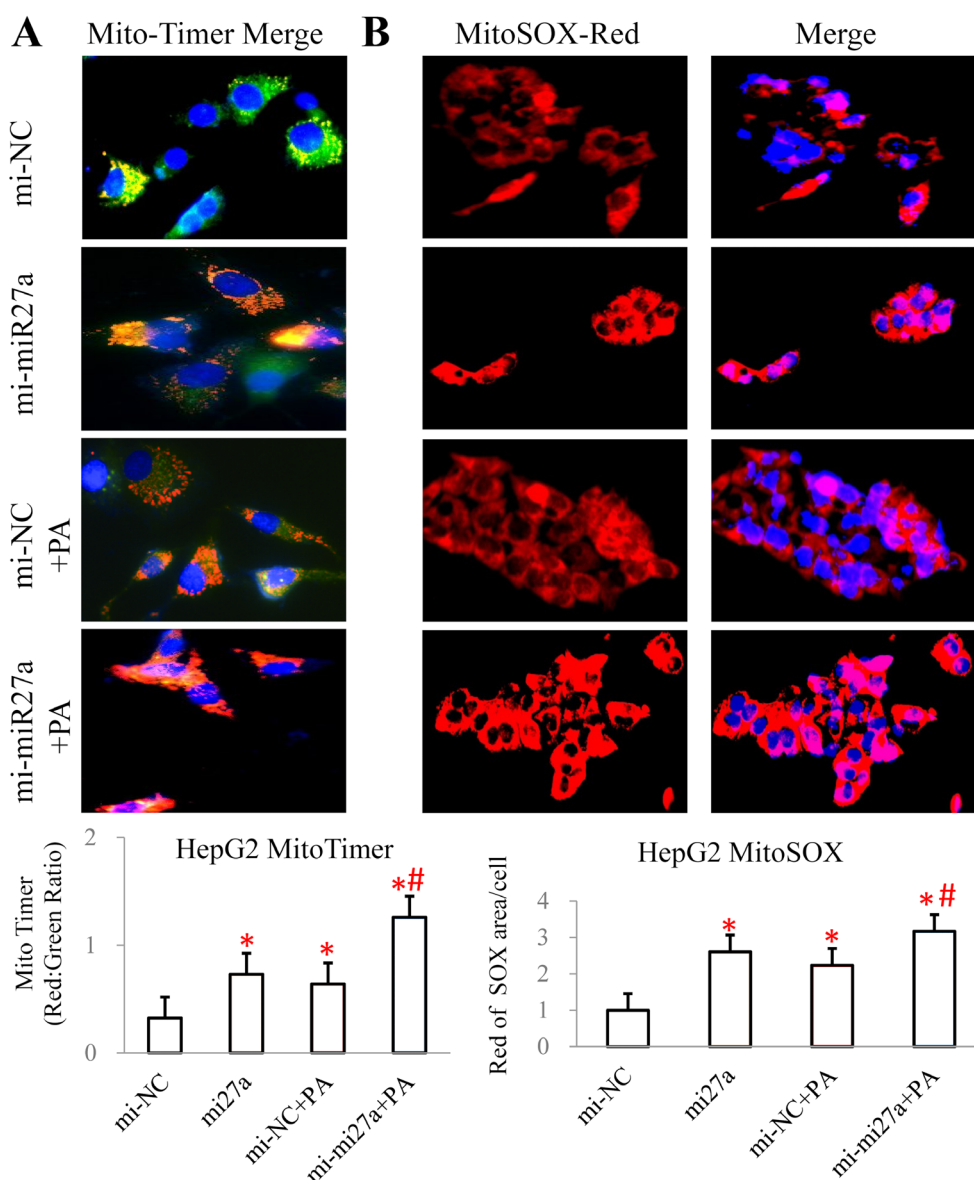
Figure 2. Obesity-associated miR-27a notably suppressed mitochondrial function in liver cancer cells. mi-NC, mi-miR27a, mi-NC+PA, and mi-miR27a+PA groups were established in HepG2 cells. A) Representative images and quantitative analysis of Mito-Timer assay results are displayed (blue IF represents nuclei; green IF represents healthy young mitochondria; red IF represents damaged old mitochondria). B) Representative images and quantitative analysis of Mito-SOX staining results are shown (blue IF: nuclei; red IF: mitochondrial ROS production). *Indicates vs. the mi-NC group, p<0.05, #indicates vs. the mi-miR-27a group, p<0.05

27a+PA and mi-miR-27a+PA+ov-BTG2 (overexpression of BTG2). BTG2 could reverse the effects of miR-27a+PA on lipid accumulation (Figure 6A, Supplementary Figure S1C), increased invasion (Figure 6B), and increased proliferation (Figure 6C). Similarly, BTG2 could reverse the effects of miR-27a+PA on mitochondrial dysfunction, including the accumulation of damaged mitochondria (Figure 6D) and increased oxidative levels (Figure 6E). Therefore, mi-miR-27a+PA could not perform oncogenic functions or induce mitochondrial dysfunction when BTG2 was overexpressed in liver cancer cells.

Discussion

Obesity is well acknowledged as a major risk factor for malignancies, particularly for HCC, mainly due to its close association with NAFLD. Recently, overwhelming evidence has supported a risk relationship between obesity and HCC [25, 26].

Currently, a novel class of regulatory molecules, adipocyte-derived miRNAs, have become a research hotspot in exploring the progression of HCC [9]. miR-27a, a well-known "onco-miRNA", has been identified as an adipocyte
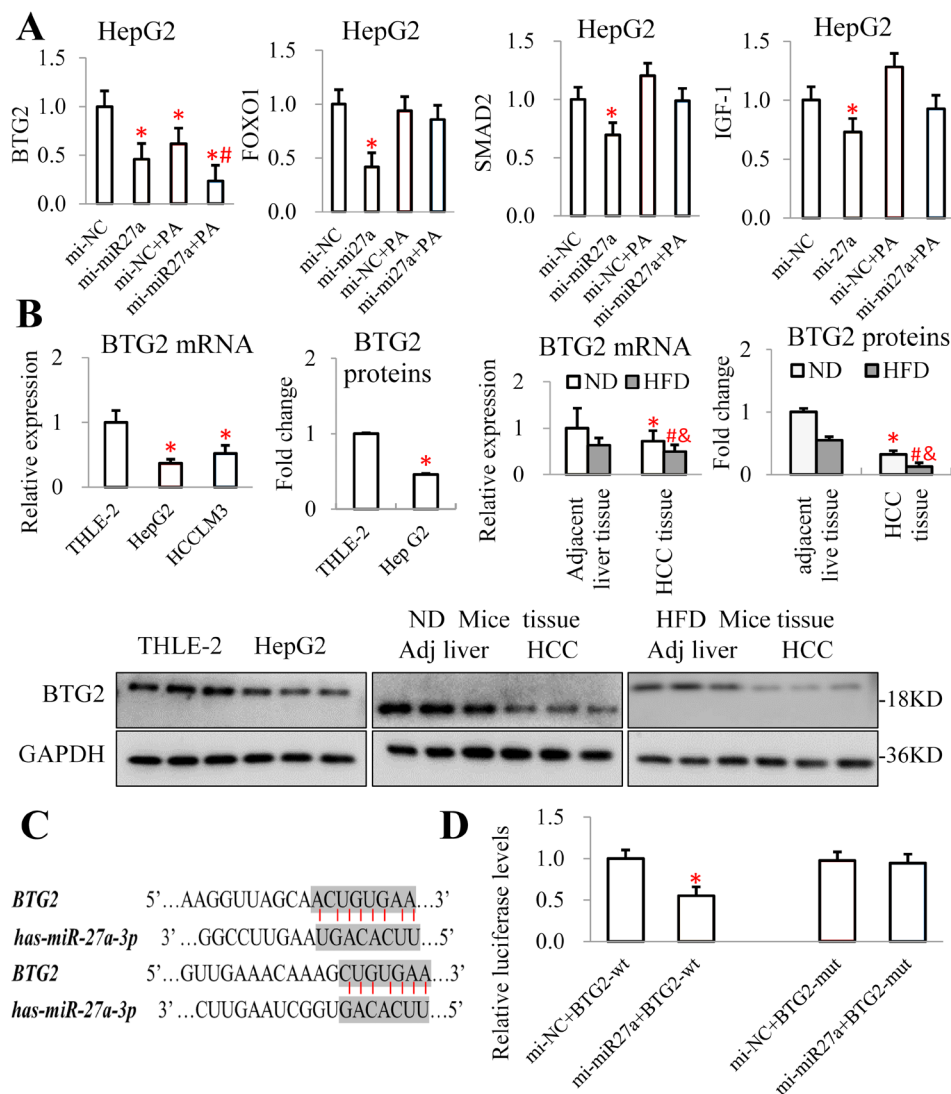
Figure 3. BTG2 was identified as a key target and was negatively regulated by obesity-associated miR-27a in HCC. A) The expression of BTG2, IGF-1, SMAD2, and FOXO1 mRNA was detected via qPCR in HepG2 cells. *Indicates vs. the mi-NC group, p<0.05, #indicates vs. the mi-miR-27a group, p<0.05. **B)** The BTG2 mRNA and protein expression were analyzed in cell lines (THLE-2, HepG2, HCCLM3) and liver tissues from HCC mice (ND and HFD groups) via qPCR and western blotting. *Indicates vs. THLE-2 cells or adjacent liver tissue in the ND group, p<0.05; #indicates vs. adjacent liver tissue from the HFD group, p<0.05; & indicates vs. HCC tissue from the ND group, p<0.05. **C)** Two binding sites for miR-27a (nt361-368 and nt1832-1838) were identified in the BTG2 3'UTR. **D)** A luciferase reporter assay revealed that mi-miR-27a decreased the luciferase activity of the BTG2-wt reporter. *Indicates vs. the mi-NC+BTG2-wt group, p<0.05
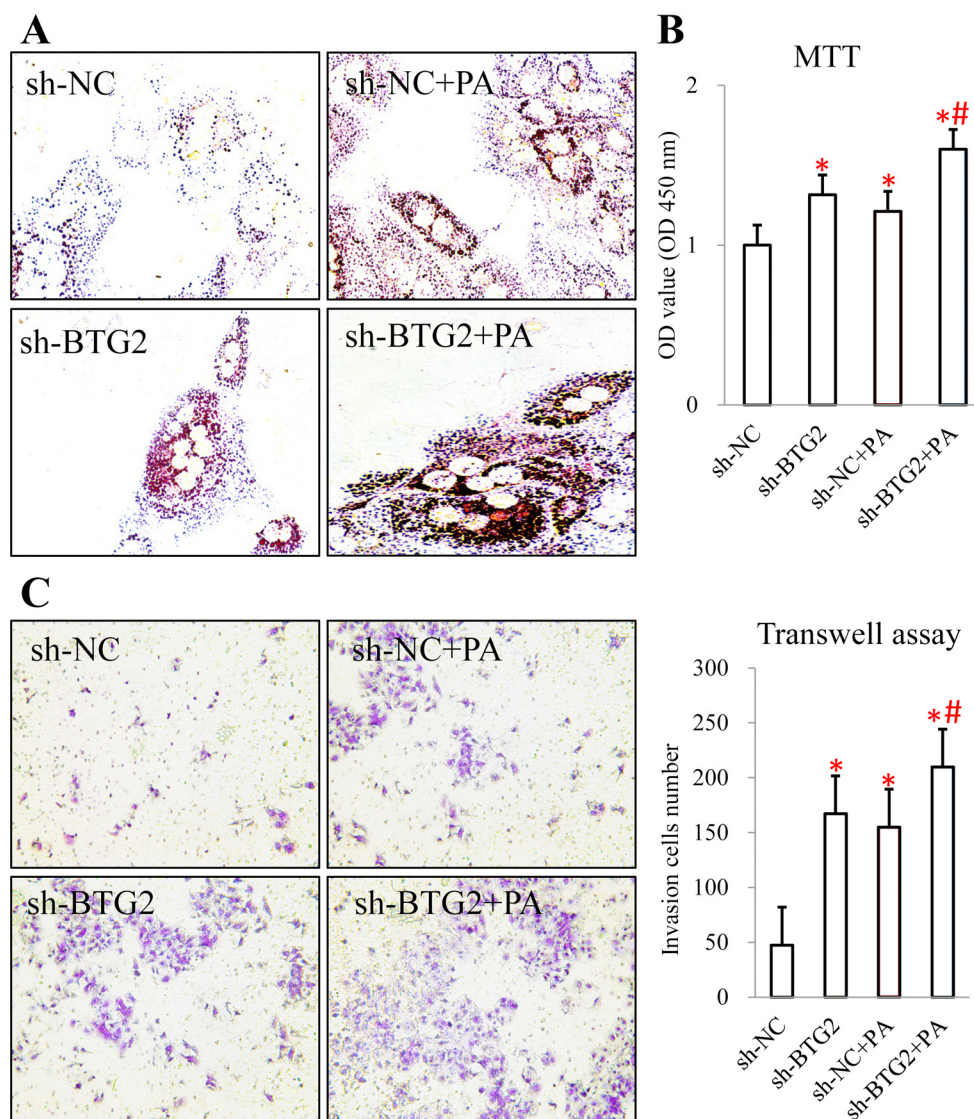
Figure 4. Downregulation of BTG2 evidently promoted lipid accumulation, proliferation, and invasion of obesity-related liver cancer cells. Four groups (sh-NC, sh-BTG2, sh-NC, sh-NC+PA, and sh-BTG2+PA) were established in PHCs and HepG2 cells. A) ORO staining revealed lipid enrichment in PHCs. B) Cellular viability was detected with MTT assays. C) Cell invasion ability was examined using Transwell assays. *Indicates vs. the sh-NC group, p<0.05, #indicates vs. the sh-BTG2 group, p<0.05

tissue-derived miRNA [10]. Our data verified that miR-27a expression was significantly elevated in liver cancer cells and HCC tissues of mice, especially under obesity conditions. The evident oncogenic functions of miR-27a were further identified in our study, including promotion of lipid accumulation, proliferation, and invasion in liver cancer cells. Moreover, the above effects of miR-27a were significantly strengthened in the presence of obesity *in vitro*. Mitochondrial dysfunction and ROS overproduction have been suggested to be associated with the growth of HCC [27]. miR-27a also markedly accelerated mitochondrial dysfunction (including mitochondrial aging and ROS overproduction) in liver

cancer cells in our study. Furthermore, the mitochondrial impairment induced by miR-27a was markedly strengthened under obesity conditions. Therefore, damaged mitochondrial function is positively related to the oncogenic activity of obesity-associated miR-27a, including enhanced lipid accumulation, proliferation, and invasion in liver cancer cells.

As miRNAs usually exert biological functions by targeting downstream genes, it is necessary to identify the key target for exploring the molecular basis of obesity-associated miR-27a in HCC development. Notably, miR-27a significantly downregulated BTG2 mRNA in HepG2 cells in obesity
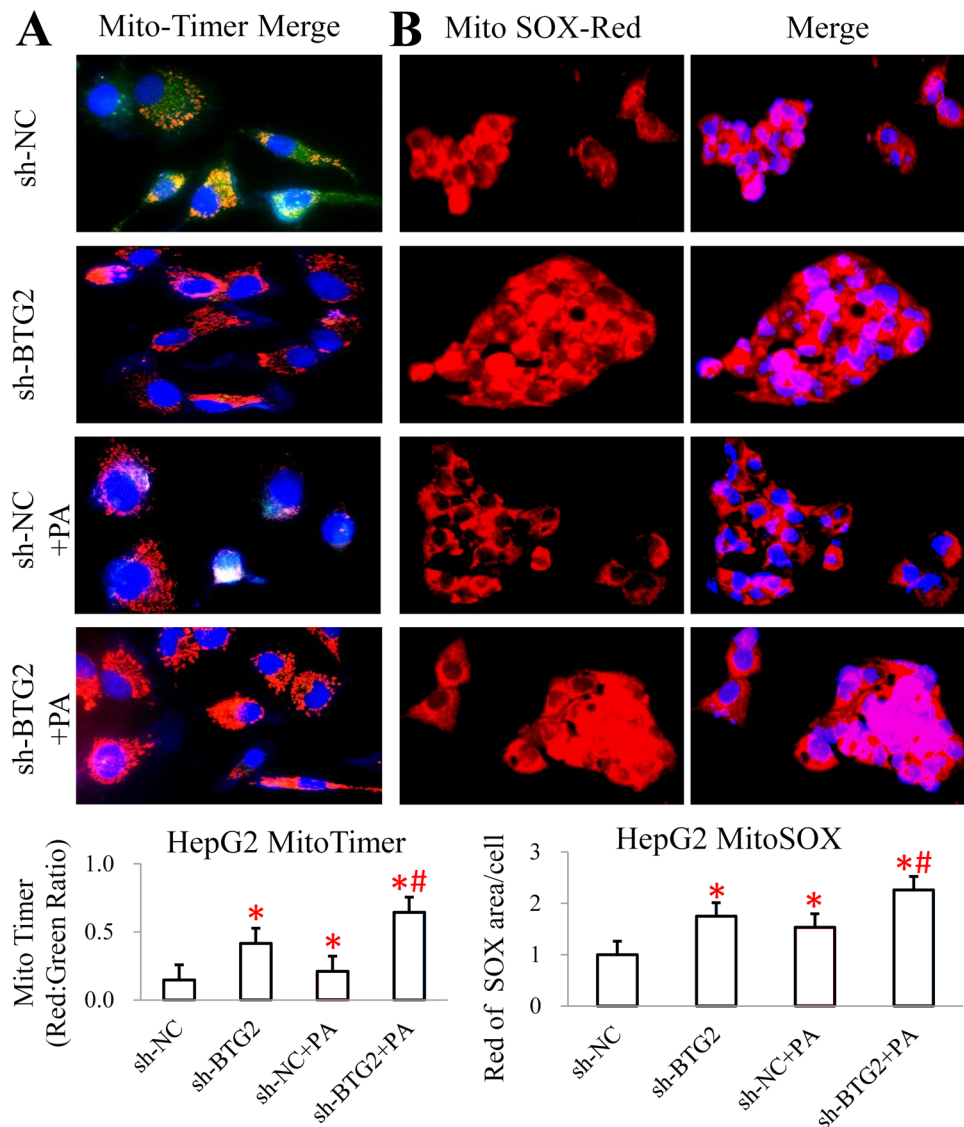
Figure 5. Suppression of BTG2 resulted in striking mitochondrial dysfunction in obesity-related liver cancer cells. Four groups (sh-NC, sh-BTG2, sh-NC, sh-NC+PA, and sh-BTG2+PA) were established in HepG2 cells. A) Representative images and the ratio values of Mito-Timer IF indicating mitochondrial turnover are displayed. B) Representative images and quantification of mitochondrial ROS production via Mito-SOX staining are shown. *Indicates vs. the sh-NC group, $p<0.05$, #indicates vs. the sh-BTG2 group, $p<0.05$

conditions. Their direct interaction was confirmed by bioinformatics analysis and luciferase activity experiments. Therefore, BTG2 is a direct target and is negatively modulated by obesity-associated miR-27a in liver cancer cells. Thus, we selected BTG2 for further study of the mechanism of obesity-associated miR-27a in HCC.

BTG2, a member of the BTG/TOB family of antiproliferation proteins, regulates a range of cellular functions, including protecting mitochondrial function [24], resisting lipid accumulation [28], and inhibiting tumor proliferation [29]. Consistently, our study identified a clear decrease in BTG2 mRNA and protein levels in HCC *in vitro* and *in vivo*. Interestingly, obesity had a markedly negative impact on BTG2 mRNA and protein expression. In addition, inhibition of BTG2 was found to act as a tumor promoter, notably triggering lipid accumulation, proliferation, and invasion, which are related to mitochondrial damage, in HCC cells. These important functions of BTG2 inhibition were also reinforced under obesity conditions *in vitro*. Then, the restoration of BTG2 was found to reverse the oncogenic function of miR-27a and the mitochondrial dysfunction induced by miR-27a overexpression in obesity-related liver cancer cells.
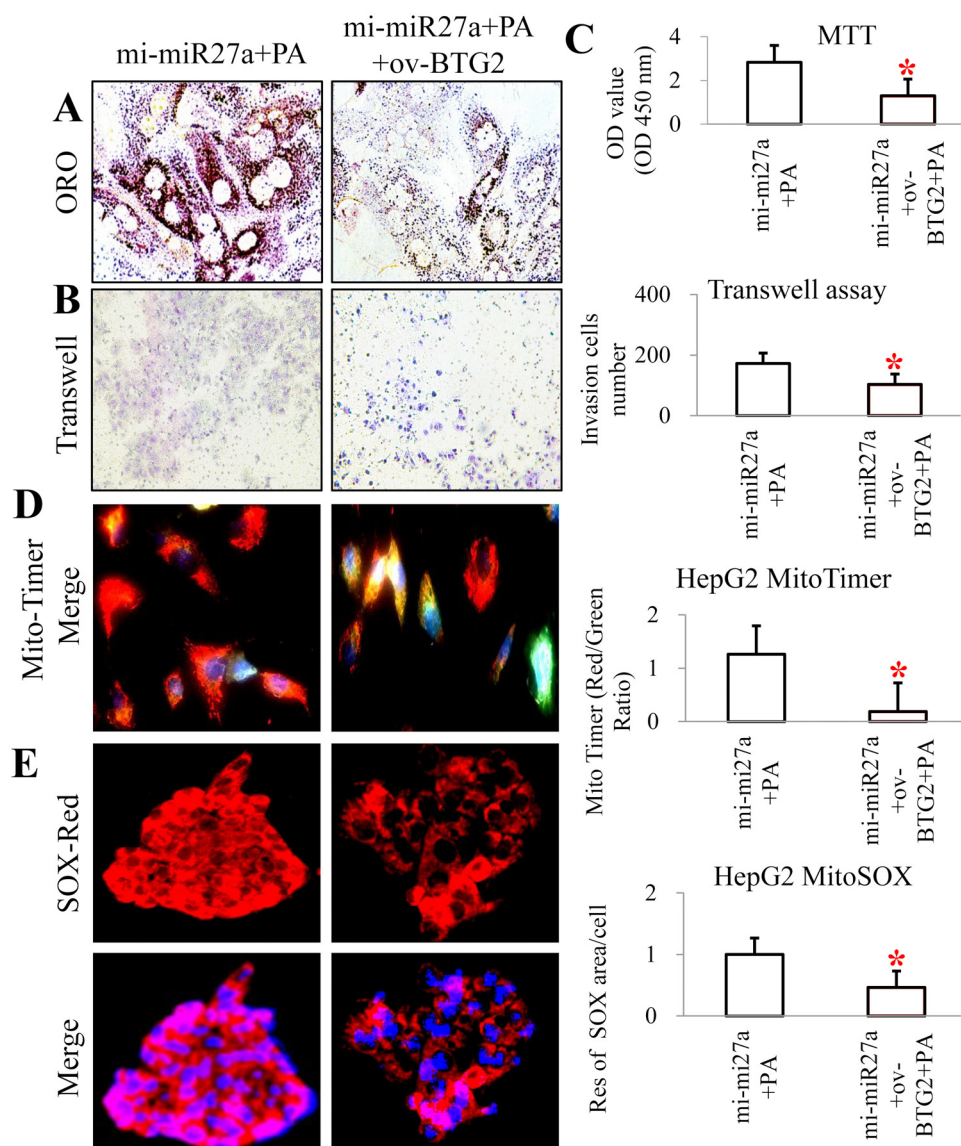
Figure 6. Obesity-associated miR-27a did not aggravate HCC progression or impair mitochondria in the presence of BTG2 overexpression *in vitro*. Two groups (mi-miR-27a+PA and mi-miR-27a+PA+ov-BTG2) were established in PHCs and HepG2 cells. A) ORO staining revealed lipid enrichment in PHCs. B) Cell invasion was examined using Transwell assays. C) Cell viability was detected with MTT assays. D) Representative images and quantification of MitoTimer IF staining were displayed. E) Representative images and quantification of Mito-SOX staining are shown. *Indicates vs. the mi-miR-27a+PA group, p<0.05

Collectively, obesity-associated miR-27a acts as an oncogene by suppressing BTG2 in HCC.

The specific role of the miR-27a-BTG2 axis in obesity-related HCC was first revealed in our study. The axis in which miR-27a negatively regulates BTG2 was confirmed to promote lipid accumulation, growth, and invasion in HCC cells, which was positively correlated with mitochondrial dysfunction in obesity-related HCC. Furthermore, we hypothesized that the obesity-associated miR-27a-BTG2 axis might play an oncogenic function in HCC by initiating mitochondrial dysfunction. BTG2 can induce programmed

cell death through direct binding to PIN-1 (protein-interacting NIMA), a master regulator of mitochondrial apoptosis. Upon BTG2 binding, PIN-1 translocates from the nucleus to the cytoplasm, where it triggers mitochondrial membrane depolarization [30]. BTG2 further inhibits adipocyte differentiation by regulating Stat3 signaling [28]. Moreover, BTG2 inhibits the proliferation and metastasis of cancer cells by suppressing the PI3K/AKT pathway [31]. Therefore, BTG2 acts as an oncosuppressor gene in cancer cells by regulating mitochondrial apoptosis and controlling cancer progression.

In conclusion, our results provide novel insight into the obesity-associated miR-27a-BTG2 axis as a molecular basis of HCC. In detail, obesity-associated miR-27a acts as an oncogene that promotes lipid accumulation, proliferation, and invasion by suppressing BTG2-mediated mitochondrial dysfunction in HCC. Thus, our results provide useful information for targeting the obesity-associated miR-27a-BTG2 axis as a new therapeutic strategy.

Supplementary information is available in the online version of the paper.

References

[1] SIEGEL RL, MILLER KD, JEMAL A. Cancer statistics, 2020. CA Cancer J Clin 2020; 70: 7–30. https://doi.org/10.3322/caac.21590

[2] ISLAMI F, GODING SAUER A, MILLKER KD, SIEGEL RL, EDEWA SA et al. Proportion and number of cancer cases and deaths attributable to potentially modifiable risk factors in the United States. CA Cancer J Clin 2018; 68: 31–54. https://doi.org/10.3322/caac.21440

[3] WELZEL TM, GRAUBARD BI, ZEUZEM S, El-SERAG HB et al. Metabolic syndrome increases the risk of primary liver cancer in the United States: a study in the SEER-Medicare database. Hepatology 2011; 54: 463–471. https://doi.org/10.1002/hep.24397

[4] PETRUCCIANI N, GUGENHEIM J. Molecular pathways between obesity, non-alcoholic steatohepatitis (NASH) and hepatocellular carcinoma (HCC). Hepatobiliary Surg Nutr 2019; 8: 395–397. https://doi.org/10.21037/hbsn.2019.03.13

[5] LIN L, DING Y, WANG Y, WANG Z, YIN X et al. Functional lipidomics: Palmitic acid impairs hepatocellular carcinoma development by modulating membrane fluidity and glucose metabolism. Hepatology 2017; 66: 432–448. https://doi.org/10.1002/hep.29033

[6] FU H, TANG B, LANG J, DU Y, CAO B et al. High-fat diet promotes macrophage-mediated hepatic inflammation and aggravates diethylnitrosamine-induced hepatocarcinogenesis in mice. Front Nutr 2020; 7: 585306. https://doi.org/10.3389/fnut.2020.585306

[7] MALIK SA, ACHARYA JD, MEHENDALE NK, KAMAT SS, GHASKADB SS et al. Pterostilbene reverses palmitic acid mediated insulin resistance in HepG2 cells by reducing oxidative stress and triglyceride accumulation. Free Radic Res 2019; 53: 815–827. https://doi.org/10.1080/10715762.2019.1635252

[8] GAN L, LIU Z, SUN C. Obesity linking to hepatocellular carcinoma: A global view. Biochim Biophys Acta Rev Cancer 2018; 869: 97–102. https://doi.org/1016/j.bbcan.2017.12.006

[9] FERRANTE SC, NADLER EP, PILLAI DK, HUBAL MJ, WANG Z et al. Adipocyte-derived exosomal miRNAs: a novel mechanism for obesity-related disease. Pediatr Res 2015; 77: 447–454. https://doi.org/10.1038/pr.2014.202

[10] YU Y, DUH, WEI S, FENG L, LI J et al. Adipocyte-Derived Exosomal MiR-27a Induces Insulin Resistance in Skeletal Muscle Through Repression of PPARγ. Theranostics 2018; 8: 2171–2188. https://doi.org/10.7150/thno.22565

[11] CHEN Y, ZHANG F, ZHAO Y, HE K, ZHENG X et al. Obesity-associated miR-27a upregulation promotes hepatocellular carcinoma metastasis through suppressing SFRP1. Onco Targets Ther 2018; 11: 3281–3292. https://doi.org/10.2147/OTT.S162978

[12] KANG T, LU W, XU W, ANDERSON L, BACANAMWO M et al. MicroRNA-27 (miR-27) targets prohibitin and impairs adipocyte differentiation and mitochondrial function in human adipose-derived stem cells. J Biol Chem 2013; 288: 34394–3402. https://doi.org/10.1074/jbc.M113.514372

[13] LV X, YU H, ZHANG Q, HUANG Q, HONG X et al. SRXN1 stimulates hepatocellular carcinoma tumorigenesis and metastasis through modulating ROS/p65/BTG2 signalling. J Cell Mol Med 2020; 24: 10714–10729. https://doi.org/10.1111/jcmm.15693

[14] SHAO M, SHAN B, LIU Y, DENG Y, YAN C, et al. Hepatic IRE1α regulates fasting-induced metabolic adaptive programs through the XBP1s-PPARα axis signalling. Nat Commun 2014; 5: 3528. https://doi.org/10.1038/ncomms4528

[15] LI W, LI Y, SIRAJ S, JIN H, FAN Y et al. FUN14 Domain-Containing 1-Mediated Mitophagy Suppresses Hepatocarcinogenesis by Inhibition of Inflammasome Activation in Mice. Hepatology 2019; 69: 604–621. https://doi.org/10.1002/hep.30191

[16] WILLIAMS JA, ZHAO K, JIN S, DING WX. New methods for monitoring mitochondrial biogenesis and mitophagy in vitro and in vivo. Exp Biol Med (Maywood) 2017; 242: 781–787. https://doi.org/10.1177/1535370216688802

[17] HSIAO YP, LAI WW, WU SB, TSAI CH, TANG SC et al. Triggering apoptotic death of human epidermal keratinocytes by malic Acid: involvement of endoplasmic reticulum stress- and mitochondria-dependent signaling pathways. Toxins (Basel) 2015; 7: 81–96. https://doi.org/10.3390/toxins7010081

[18] LI WQ, YU HY, ZHONG NZ, HOU LJ, LI YM et al. miR-27a suppresses the clonogenic growth and migration of human glioblastoma multiforme cells by targeting BTG2. Int J Oncol 2015; 46: 1601–1608. https://doi.org/10.3892/ijo.2015.2843

[19] ZHANG LY, CHEN Y, JIA J, ZHU X, HE Y et al. MiR-27a promotes EMT in ovarian cancer through active Wnt/β-catenin signalling by targeting FOXO1. Cancer Biomark 2019; 24: 31–42. https://doi.org/10.3233/CBM-181229

[20] CHEN Y, ZHANG X, AN Y, LIU B, LU M. LncRNA HCP5 promotes cell proliferation and inhibits apoptosis via miR-27a-3p/IGF-1 axis in human granulosa-like tumor cell line KGN. Mol Cell Endocrinol 2020; 503: 110697. https://doi.org/10.1016/j.mce.2019.110697

[21] CHAE DK, BAN E, YOO YS, KIM EE, BAIK JH et al. MIR-27a regulates the TGF-β signaling pathway by targeting SMAD2 and SMAD4 in lung cancer. Mol Carcinog 2017; 56: 1992–1998. https://doi.org/10.1002/mc.22655

[22] PARK TJ, KIM JY, OH SP, KANG SY, KIM BW et al. TIS21 negatively regulates hepatocarcinogenesis by disruption of cyclin B1-Forkhead box M1 regulation loop. Hepatology 2008; 47: 1533–1543. https://doi.org/10.1002/hep.22212

[23] GAN M, SHEN L, WANG S, GUO Z, ZHENG T et al. Genistein inhibits high fat diet-induced obesity through miR-222 by targeting BTG2 and adipor1. Food Funct 2020; 11: 2418–2426.

[24] LAU D, BADING H. Synaptic activity-mediated suppression of p53 and induction of nuclear calcium-regulated neuroprotective genes promote survival through inhibition of mitochondrial permeability transition. J Neurosci 2009; 29: 4420–4429. https://doi.org/10.1002/hep.22212

[25] LARSSON SC, WOLK A. Overweight, obesity and risk of liver cancer: a meta-analysis of cohort studies. Br J Cancer 2007; 97: 1005–1008. https://doi.org/10.1038/sj.bjc.6603932

[26] RENEHAN AG, TYSON M, EGGER M, HELLER RF, ZWAHLEN M. Body-mass index and incidence of cancer: a systematic review and meta-analysis of prospective observational studies. Lancet 2008; 371: 569–578. https://doi.org/10.1016/S0140-6736(08)60269-X

[27] GENG X, GENG Z, LI H, ZHANG Y, LI J et al. Over-expression of TFB2M facilitates cell growth and metastasis via activating ROS-Akt-NF-κB signalling in hepatocellular carcinoma. Liver Int 2020; 40: 1756–1769. https://doi.org/10.1111/liv.14440

[28] KIM S, HONG JW, PARK KW. B cell translocation gene 2 (Btg2) is regulated by Stat3 signaling and inhibits adipocyte differentiation. Mol Cell Biochem 2016; 413: 145–153. https://doi.org/10.1007/s11010-015-2648-z

[29] ZHANG Z, CHEN C, WANG G, YANG Z, SAN J, et al. BTG2 Is Down-Regulated and Inhibits Cancer Stem Cell-Like Features of Side Population Cells in Hepatocellular Carcinoma. Dig Dis Sci 2017; 62: 3501–3510. https://doi.org/10.1007/s10620-017-4829-y

[30] FIORI ME, VILLANOVA L, BARBINI C, ANGELIS MLD, MARIA RD. miR-663 sustains NSCLC by inhibiting mitochondrial outer membrane permeabilization (MOMP) through PUMA/BBC3 and BTG2. Cell Death Dis 2018; 9: 49. https://doi.org/10.1038/s41419-017-0080-x

[31] LI YJ, DONG BK, FAN M, JIANG WX. BTG2 inhibits the proliferation and metastasis of osteosarcoma cells by suppressing the PI3K/AKT pathway. Int J Clin Exp Pathol 2015; 8: 12410–12418.

The oncogenic miR-27a/BTG2 axis promotes obesity-associated hepatocellular carcinoma by mediating mitochondrial dysfunction

Qi SU[1,#], Zi-Xin XU[2,#], Min-Li XIONG[3], Hui-Yi LI[4], Ming-Yi XU[4,*], Sheng-Zheng LUO[2,*]

Supplementary Information

Supplementary Table S1. Information of Plasmids used in study.

	Species	Name of the carrier	Corp.	Sequence (5'-3')
mi-miR27a	human	None	Gene Pharma Co. Ltd, Shanghai, China	F:UUCACAGUGGCUAAGUUCCGC R:GGAACUUAGCCACUGUGAAUU
mi-NC	human	None	Gene Pharma Co. Ltd, Shanghai, China	F:UUUGUACUACACAAAAGUACUG R:CAGUACUUUUGUGUAGUACAAA
ov-BTG2	human	pEX-3(pGCMV/MCS/Neo)	Gene Pharma Co. Ltd, Shanghai, China	ATGAGCCACGGGAAGGGAACCGACATGCTCCCGGAGATCGCCGCC-GCCGTGGGCTTCCTCTCCAGCCTCC TGAGGACCCGGGGCTGCGTGAGCGAGCAGAGGCTTA-AGGTCTTCAGCGGGGCGCTCCAGGAGGCACTCAC AGAGCACTACAAACACCACTGGTTTCCCGAAAAGCCGTC-CAAGGGCTCCGGCTACCGCTGCATTCGCATC AACCACAAGATGGACCCCATCATCAGCAGGGTGGCCAGCCAGATCG-GACTCAGCCAGCCCCAGCTGCACC AGCTGCTGCCCAGCGAGCTGACCCTGTGGGTGGACCCCTATGAGGT-GTCCTACCGCATTGGGGAGGACGG CTCCATCTGCGTCTTGTACGAGGAGGCCCCACTGGCCGCCTCCTGT-GGGCTCCTCACCTGCAAGAACCAA GTGCTGCTGGGCCGGAGCAGCCCCTCCAAGAACTACGTGATG-GCAGTCTCCAGCTAG
sh-BTG2	human		Gene Pharma Co. Ltd, Shanghai, China	GGACGCACTGACCGATCATTA
sh-NC	human		Gene Pharma Co. Ltd, Shanghai, China	GCTACACAAATCAGCGATTT

Supplementary Table S2. The sequence of related genes for qPCR.

Genes	Host	Forward (5'–3')	Reverse (5'–3')	NCBI Gene ID/ Primer GenBank ID	GenBank accession	Amplicon Size
miR27a	Human	GCGCGTTCACAGTGGC-TAAG	AGTGCAGGGTCCGAGGTATT			
miR27a-RT	Human	GTCGTATCCAGTG-CAGGGTCCGAGGTAT TCGCACTGGATACGACGC-GGAA		407081		
miR27a	Mouse	GCGCGTTCACAGTGGC-TAAG	AGTGCAGGGTCCGAGGTATT			
miR27a-RT	Mouse	GTCGTATCCAGTG-CAGGGTCCGAGGTAT TCGCACTGGATACGACGC-GGAA		387220		
U6	Human	GCTCGCTTCGGCAGCA-CATATAC	AGTGCAGGGTCCGAGGTATT			
U6-RT	Human	GTCGTATCCAGTG-CAGGGTCCGAGGTAT TCGCACTGGATACGA-CAAAATATGG		26827		
U6	Mouse	GCTTCGGCAGCACATATAC-TAAAAT	CGCTTCACGAATTTGCGT-GTCAT			
U6-RT	Mouse	GTCGTATCCAGTG-CAGGGTCCGAGGTAT TCGCACTGGATACGA-CAAAATATGG		67207		
GAPDH	Human	ACAACTTTGGTATCGTG-GAAGG	GCCATCACGCCACAGTTTC	2597/378404907c2	NM_001256799	101
GAPDH	Mouse	AGGTCGGTGTGAACG-GATTTG	TGTAGACCATGTAGTTGAG-GTCA	14433/6679937a1	NM_008084	123
BTG2	Human	ACGGGAAGGGAACCGA-CAT	CAGTGGTGTTTGTAGT-GCTCTG	7832/28872718c1	NM_006763	154
BTG2	Mouse	ATGAGCCACGGGAAGAGA-AC	AGCGCCCTACTGAAAACCTTG	12227/6680814a1	NM_007570	122
FOXO-1	Human	TGATAACTGGAGTA-CATTTCGCC	CGGTCATAATGGGTGAGA-GTCT	2308/133930787c2	NM_002015	80
IGF-1	Human	GCTCTTCAGTTCGTGTGT-GGA	GCCTCCTTAGATCACAGCTCC	3479/163659898c1	NM_001111283	133
SMAD2	Human	CGTCCATCTTGC-CATTCACG	CTCAAGCTCATCTAATC-GTCCTG	4087/118572580c1	NP_005892	182

Supplementary Table 3. The sequence of BTG2 for luciferase assay.

Genes	Forward (5'–3')	Reverse (5'–3')
BTG2-wt	CTCTAGGACAAGAGTTCTCAGTCACT<u>GTGCAAT</u>AT-GCCCCCTGGGTCCCAGGAGGGTCTACAATCCAAATTT-GTCGTAGACTT<u>GTGCAAT</u>ATATACTGTTGTGGGTTG-GAGAAAAG	TCGACTCCAACCCACAACAGTATAT<u>ATTGCAC</u>AAGTCTACGA-CAAATTTGGATTGTAGACCCTCCTGGGACCCAGGGGGCAT<u>ATT-GCAC</u>AGTGACTGAGAACTCTTGTCCTAGAGAGCT
BTG2-mut	CTCTAGGACAAGAGTTCTCAGTCACT<u>GTGCAAT</u>AT-GCCCCCTGGGTCCCAGG AGGGTCTACAATCCAAATTTGTCGTAGACTT<u>GACGTT-</u>TATATACTGTTGTGGGTTGGAGAAAAG	TCGACTCCAACCCACAACAGTATAT<u>AAACGTC</u>AAGTCTACGA-CAAATTTGGATTG TAGACCCTCCTGGGACCCAGGGGGCAT<u>ATTGCAC</u>AGTGACT-GAGAACTCTTGTCCTAGAGAGCT
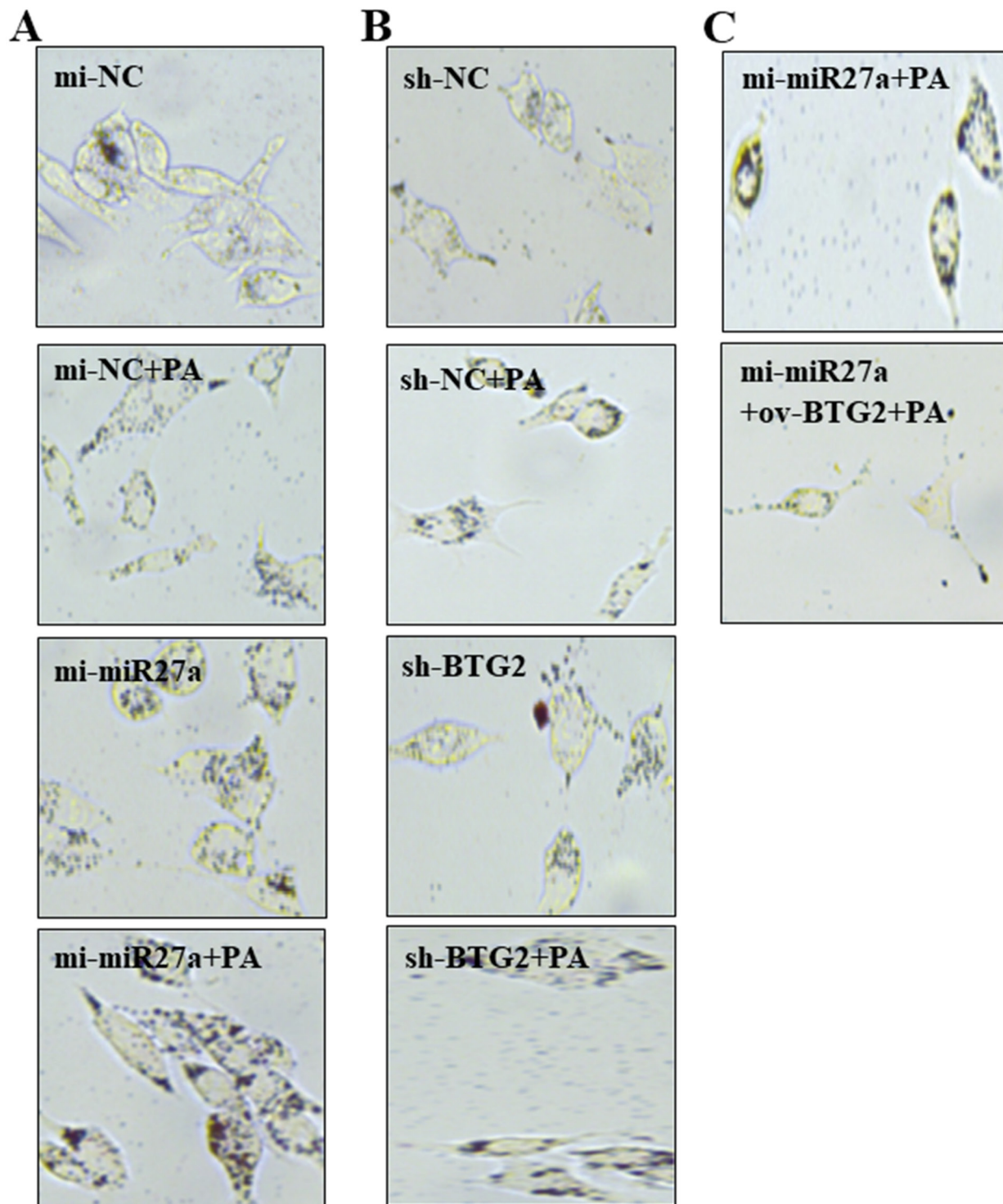
Supplementary Figure S1. Representative images of ORO staining in HepG2 cells. A) ORO staining revealed lipid enrichment in 4 groups of HepG2 cells (mi-NC, mi-miR-27a, mi-NC+PA and mi-miR27a +PA). **B)** ORO staining revealed lipid enrichment in 4 groups of HepG2 cells (sh-NC, sh-BTG2, sh-NC+PA and sh-BTG2 +PA). **C)** ORO staining revealed lipid enrichment in 2 groups of HepG2 cells (mi-miR27a +PA and mi-miR27a +ov-BTG2 +PA).